IMEKO International Conference on
Metrology for Archaeology and Cultural Heritage
Lecce, Italy, October 23-25, 2017

Comparison of two well-established 3D acquisition techniques on a small fragmental artefact of a few cubic centimeters

Adriana Bandiera[1], Francesco Meo[2], Angelo Cammalleri[2], Catia Bianco[2], Jean-Angelo Beraldin[3]

[1] Coordinamento SIBA University of Salento, Lecce (IT), adriana.bandiera@unisalento.it
[2] Department of Cultural Heritage University of Salento, Lecce (IT), francesco.meo@unisalento.it, angelo.cammalleri@studenti.unisalento.it, catia.bianco@libero.it
[3] Retired researcher (Canada)

***Abstract* –The aim of this study is to obtain 3D digital models of small and opaque ceramic fragments with 3D acquisition techniques. One of these fragments used for the experiment was retrieved during an excavation campaign at Muro Leccese, Italy. That ceramic fragment is characterised by a relatively small size (3.5 cm x 4 cm x 0.4 cm), with a slight curvature and specular paintings. We investigated the use of two well-established 3D data acquisition techniques available at the university's 3D laboratory, i.e., high resolution laser scanning and multi-view dense stereo based on polarised light. The creation of two metrically correct 3D models similar to the real artefact that are both functional and simple to display, as a result. The digital model presented us with the possibility to identify the correct inclination of the fragment in order to identify the ceramic form.**

Key words: Archaeology, laser scanning, dense-stereo, photogrammetry, polarised light, focus stacking.

I. INTRODUCTION

Archaeology is an ever-evolving scientific discipline and its study requires up-to-date technical skills, in addition to historical and humanistic knowledge. This background is mandatory and necessary in order to facilitate the understanding of archaeological digs and discoveries. In fact, interpretation of archaeological artefacts especially in fragment form are exceedingly challenging since the contours of profiles, that define the shape of an object or the traces of its modifications, are not easily recognisable. Digital models are useful media for the archaeologists giving them the opportunity to capture details, which would otherwise be nearly impossible to see with the naked eye. In the last decade or so dense stereo based on photogrammetry became an essential tool for reconstruction of digital three-dimensional (3D) models from antiquity with sub-millimeter precision.

The aim of this study is to better understand the origin of small fragments using 3D digital models, while simultaneously comparing two well-established 3D acquisition techniques available at the university's 3D laboratory.

The archaeological research conducted in Muro Leccese (LE, Italy) by the Department of Cultural Heritage of the University of Salento has addressed several areas since 2000. The latest results now allow us to draw a profile of the ancient inhabited area as a whole [1, 2, 3, 4, 5, 6, 7]. Muro Leccese's history can be divided into three phases characterised by different forms of settlement: an Iron Age village from the mid-8th to the mid-6th centuries BCE; an Archaic settlement from the second half of the 6th to the third quarter of the 4th centuries BCE and a town surrounded by an imposing wall from the late 4th to the mid-3rd centuries BCE, when Muro Leccese was almost certainly conquered after a siege and the settlement destroyed during the *bellum sallentinum* against the Romans [8, 9]. Some information on the Archaic phase has long been available [10, 11, 12], but the discovery of a black-figured cup-skyphos fragment in 2016 contributed to a better understanding of the settlement during the archaic period.

This fragment consists of a small piece of a vessel with part of the shoulder and rim. The exterior decoration of the rim consists of a horizontal black band, whereas the shoulder has a black-figured band bordered by a black line in the lower section. The subject in the scene is a deer looking backward. The animal has been identified with a silhouette drawing and with some anatomic details incised. One side, the one closest to the handle, is limited by a palmette with nine petals and an empty heart. Despite the fact that the scene is incomplete, the subject is most probably trying to escape from a satyr that is grabbing it from behind [13] or from a feline or a dog [14] such as in other representations. In terms of orientation and reconstruction of shape, the fragment is most probably a piece of a skyphos, a deep vessel for drinking wine.

Skyphoi are well attested in other Southern Italian archaic archaeological contexts, widespread in the Adriatic and less in the Tyrrhenian one [15]. They have been discovered in Apulian settlements, Ruvo di Puglia [16] or Arpi [17] and are very well attested in Messapian

settlements i.e. Cavallino, Egnazia, Lecce, Li Fani, Mesagne, Oria, Rudiae, Vaste and Muro Leccese [18, 19, 20, 21, 22]. This type of decoration is very similar to those of the lekythoi found in the sacred area of San Biagio (Metaponto), most of which identified as part of the group of the Haimon Painter [23]. The products of the Haimon Group are widely attested in several archaeological sites [24, 25].

The ceramic fragment is characterised by a relatively small size (3.5 cm x 4 cm x 0.4 cm), a slight curvature and paintings that are specular in certain orientations. The use and possibly the integration of the two 3D data sets, one from laser scanning and the other from multi-view dense stereo based on photogrammetry, are investigated in this paper. Both of these techniques rely on optical triangulation to extract 3D surface coordinates.

The steps in the documentation process of the artefacts are described in Section II with more details, i.e. from a description of the photographic session to the creation of a 3D model using both dense stereo and laser scanning. The laser scanner technique was further complemented with texture mapping from an external software package. The multi-view dense stereo technique was augmented with polarised light and a focus stacking technique. Section III explains the main results of this comparison. The two metrically correct 3D models similar to the real artefact that are both functional (identification of the ceramic form) and simple to display are shown. Concluding remarks appear in Section IV.

II. METHODOLOGY

The archaeological artefact has been analysed from both a classical archaeological identification (i.e. definition of production class, shape, color, dating) and a modern archaeological perspective (i.e. using photogrammetric and laser scanner for 3D digital modelling). The final result are two metrically correct 3D models similar to the real artefact that are both functional and simple to display. The digital model provides us the possibility to identify the correct inclination of the fragment in order to identify the ceramic form. Apart from its relatively small size, the obverse side of the fragment is composed of earth coloured and dark decorations and the reverse side has a full glossy black finish. Both sides have signs of chisel marks and striations. The lack of colour contrast and shallow curvature may cause problems for the photogrammetric acquisition technique which generally requires more depth.

A. Laser scanning

The 3D model of the artefact was created with a laser scanner from ShapeGrabber ® [26] (configuration AI300 + SG102) with a peak acquisition rate of 100 000 coordinates/s. The scanner shown on Fig. 1 is designed for high-resolution acquisitions of very small objects. It is equipped with a rotating base which allows 3D scans all around individual artefacts in a completely automatic way. This, in turn, minimizes the time handling fragile artefacts, thereby preserving them. The structure resolution (as per VDI/VDE 2617.6.1) is as follows, lateral position resolution of 0.1 mm (best level achievable) and the axial resolution which depends on the signal-to-noise ratio and laser penetration (not present here) is about 0.01 mm on a cooperative surface however because of the darker material, it varies between 0.01 mm and 0.025 mm. The rotation base has an angular resolution in the micro-radian range. InnovMetric Polyworks ® Modeler and Inspector [27] were used for 3D image alignment, modeling and data verification.

Fig. 1. Test sample positioned on top of the rotating stage. ShapeGrabber ® AI300 + SG102.

Though the scanner is based on older components, we were able to adjust the laser power in coarse increments to limit saturation. To reduce systematic errors in the raw coordinates we used post processing. The first tests were concerned with an examination the accuracy of the scanner. We applied a reduced version of the VDI/VDE 2634 and compared the results with the performance from previous years (results not reported here). The results were consistent and allowed us to proceed. Systematic errors in active 3D triangulation systems have been studied extensively [28, 29]. There are two main problems seen only at very low measurement noise levels: inter-pixel gap and abrupt depth/intensity transitions. Fig. 2a shows the result, based on synthetically shading, where a wave pattern is present particularly in the top left corner of the image. After some simple scanning steps and some post-processing, those wave patterns are reduced to an insignificant level as shown in Fig. 2b.

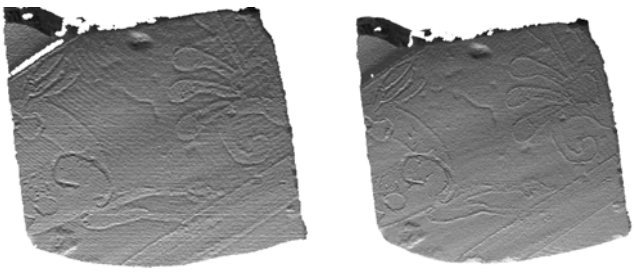

a) b)

Fig. 2. Scanner systematic errors compensation: a) wave pattern due to inter-pixel gap (top left corner of artefact), b) result of the processing to reduce the wave pattern.

It is interesting to note that the same procedure has reduced the effect of systematic errors due to abrupt changes in intensity contrasts. We proceeded in the creation of a 3D model using a series of 3D images processed by our procedure. The following figure depicts the final 3D model of the artefact.

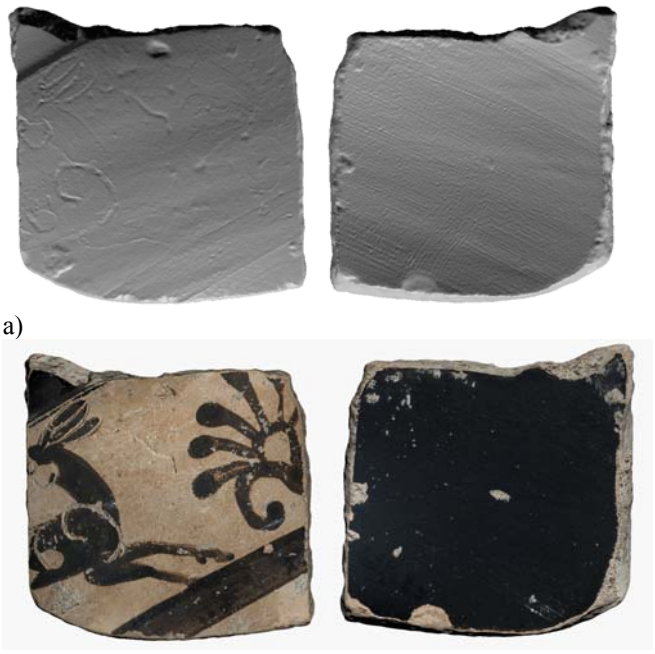

a)

b)

Fig. 3. Final 3D model: a) obverse and reverse sides shown with synthetic shading, b) colour mapped 3D model.

The four striations (top left of front view) on Fig. 3a that are quasi-parallel measure about 5.1mm in length and their width is about 0.3 mm. The lateral sampling of 0.1 mm was just enough to see those striations (tool marks) but may limit the interpretation of a possible tool that created them. The depth (axial) uncertainty of about 0.01 mm seems sufficient to measure the depth left by a particular tool. We now look at multi-view dense stereo as a possible solution to this loss of lateral resolution.

B. Multi-view dense stereo

In our multi-view dense-stereo procedure, it was first used with a SLR medium-quality photographic camera with either a 60 mm or 80 mm macro lens. These are readily available at the 3D laboratory. The experiments conducted have highlighted the issues directly related to the resolution, field of view, depth of field and stand-off distance of the two lenses.

The 60-mm macro lens has produced a higher lateral resolution and has been easier to use, i.e., larger stand-off distance. Furthermore, results using a National Bureau of Standards 1010A resolution pattern has revealed that a lateral (position) resolution of about 25 μm (200 cycles/mm) could be achieved in the conditions present in our laboratory. This result confirmed that lateral resolution could be improved over the laser scanner described in the previous section.

Considering the size of the artefacts, it was necessary to use macro photography. Keeping a high level of lateral resolution would be at the expense of depth of field (DOF) in a traditional set-up. For this reason, we investigated ways to improve the DOF while keeping a fairly constant lateral resolution. Increasing the f-number of the DSLR camera lens is a possibility but found to be insufficient in our experiment. For a given f-number, one can calculate and optimum high lateral resolution, large DOF and minimal diffraction effects. Furthermore, the choice of a method is also dictated by the cost of the extra equipment required and the ease of use in the event that the imaging system would be deployed on-site. In fact, adequate lateral resolution and the extra cost were the major factors in this project. Total person-hours and measurement time are not critical at the moment in the project.

A survey of techniques to extend the DOF of an artefact's image that was the size targeted in this paper or to create a 3D representation directly from stacked images has identified the following techniques: depth-from-defocus using a liquid lens (direct method) [30], tilt–shift photography [31] also known as the Scheimpflug principle often used with laser scanning, wave-front coding, plenoptic cameras based on a micro-lens array, colour apodization and focus-stacking (by focus-bracketed images). The cost of liquid lens objective precluded its use in our proposed system. The same conclusion for a tilt–shift lens, plenoptic cameras and colour apodization. Wave-front coding for extending depth of field imaging systems was first proposed by Cathey and Dowski [32]. The method can extend the depth of field of an imaging system by a factor of 5-10 or more compared to conventional optical imaging system. A custom-made optical element is required and hence is rejected as a solution. To minimise costs, focus stacking was used in order to extend the depth of field of the images used by the multi-view dense stereo package [33]. The focus stacking software was used as a demo from a commercial site [34].

The next step was to design the vision system or here called the optical arrangement. A dark field lighting arrangement was selected in order to emphasize shape and contours. Fig. 4 shows the basic optical arrangement which is often employed for surface defect detections applications. The re-focusing was performed by translating the DSLR camera manually along a graduated scale. To manage the radiated heat from halogen lamps effectively, LED-based lighting was used. LED PAR (Parabolic aluminized reflector)-20 were purchased in a low-end hardware store. These compact lamps are limited to about 75W equivalent power or about 8W actual power consumption and 600 lm of luminous flux.

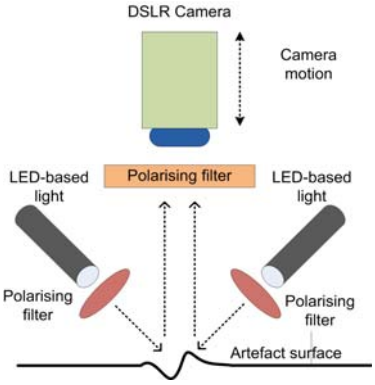

Fig. 4. Diagram showing the basic optical arrangement based on dark field lighting.

The painted surface of the artefact (i.e. the drawings with dark paint) presented some challenges. It was sometimes very dark and often specular (also known as glare). A modification of the illumination had to considered. Two types of polarising filters commercially available can be used. These are linear and circular polarising filters. They produce the same photographic effect in a digital image, i.e., reduce or even illuminate specular reflections but the metering and auto-focus sensors in many cameras will not work properly with linear polarisers. By the way, here we use polarised light to reject glare and not to estimate surface normal. We selected circular polarising filters as these were already available in the 3D laboratory.

The following figure shows an example of the glare rejection capability of optical arrangement. To compensate for the loss of the 2 stops inherent with the use of polarisation filters, the exposure time was increased. This increase in image capture was not significant compared to the time it takes to compute a 3D model with our commercial multi-view dense-stereo software.

a) b)

Fig. 5. Effect of polarisers: a) without polarised light and polarising filters, b) with the polarisers mounted in the optical arrangement based on dark field lighting. Exposure time was increased in the second image.

The equipment is listed in the table below along with some specifications. Optimal aperture was computed using a 2×pixel pitch for the circle of confusion (CoC), a magnification of 0.32 and a term for diffraction. The calculations yielded an aperture of 8.55, therefore f8 was selected. At a near field distance of 248 mm, the DOF is about 3.4 mm and the lateral resolution is about 0.02 mm. This last value is in accordance with the 1010A resolution pattern results presented earlier. According to the web site DXOMARK [35], for a f8 aperture, the chromatic aberrations of the Micro Nikkor 60mm f/2.8D is about 0.01 mm, vignetting is minimal and image sharpness is optimal. The value selected for the CoC seems to be reasonable. In accordance with the Rayleigh criterion which is a usual term when using laser beams [36], the DOF of the SG scanner is about 94 mm which is larger than the DOF of the camera-lens system used here. i.e. 3.4 mm. If it were possible to reduce in half the laser line width, the DOF would be 5.9 mm. The depth of field for a laser system is proportional to the square of the spot size. This is to say that with imaging systems laser or not, at short range distance, small values of the lateral resolution come at the expense of the DOF.

Table 1. Equipment with some specifications.

DSLR	**Lens**	**LED**	**Polarisers**
Nikon D3	Micro Nikkor 60mm f/2.8D	PAR 20	Circular 1X-2X
36 x 23.9 mm CMOS sensor	Close-range-correction. Multi-coated.	600 lm Daylight 5000K	Diameter 62, 77 mm
8.45µm pixel pitch	closest focus distance front of the lens at the	6 Watts	About 35 euros

III. RESULTS AND INTERPRETATION

Here we compare the accuracy of the two models using two criteria: structure resolution and form error. The structure resolution especially the lateral resolution is much better with the multi-view dense stereo method. The following figures show the results on a number of incisions.

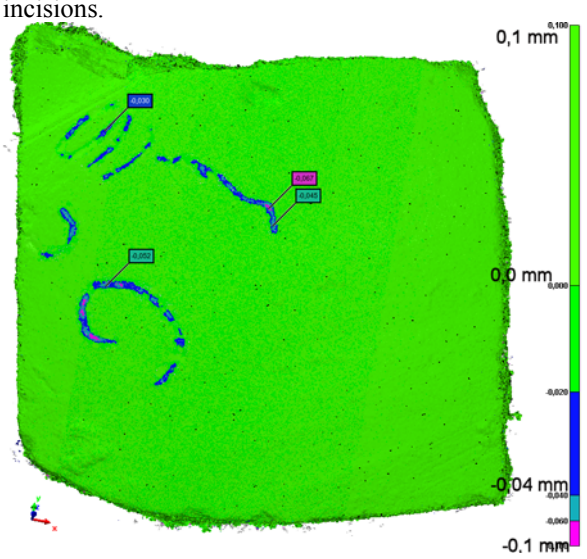

Fig. 6. Extraction of the main incisions on the digital 3D model created with Photoscan.

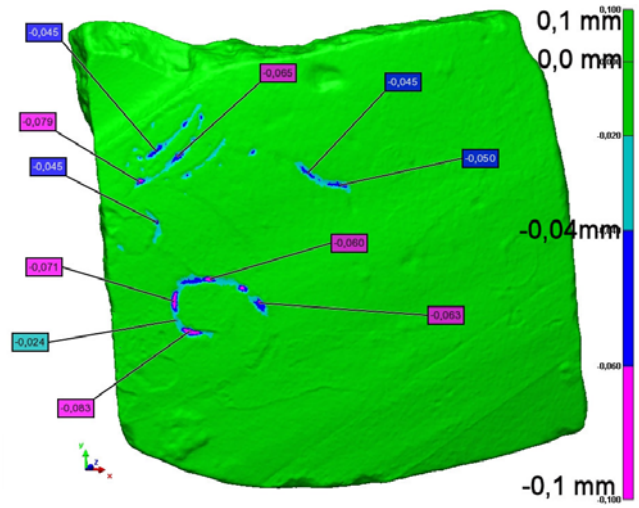

Figure 7 Extraction of the main incisions on the digital 3D model created with the laser scanner.

A comparison of the two models yielded a negligible form error so results were not included here for the sake of brevity.

The model was oriented using Autodesk 3DS Max and two parallel planes aligned with the decorations.

Figure 8. Rendering showing the two parallel planes used to align the artefact with respect to a virtual cup.

Two sections were drawn, one on the top portion and one at the bottom. From the revolution of those sections, a circle placed on the top of the virtual cup was obtained with an estimated maximum diameter of 130 mm.

Figure 9. Creation of a virtual cup from sections of the 3D digital model.

The lack of the foot makes difficult to identify its class [37], even if it is possible to hypothesize it is a K2 or K3 of the Ure type [38].

IV. CONCLUSION

Digital 3D imaging was an indispensable element for ceramic recognition and reconstruction of the exact diameter estimation. The process of acquisition of digital 3D images by a laser scanner was analyzed. The acquisition speed for this type of instrument allows for a quicker way to generate a digital 3D model. The difficulties originate from setting the best lateral resolution, the appearance of low level 3D systematic errors at close range and dealing with saturation issues due to the artifact surface reflectance. Similar concerns were dealt with in the multi-view dense stereo method. The use of polarised light and focus stacking enhanced this modeling technique and made it usable for the present context. Image acquisition automation would be required however.

In the future, we may look to integrate those two acquisition methods for increasing the structure resolution. This has been successfully implemented for small coins by combining fine photometric detail derived from a set of photographic images with accurate geometric data from a 3-D laser scanner [39].

V. ACKNOWLEGEMENTS

Many thanks to Andrea Padovani (Opto3) for his advice with Polyworks.

VI. REFERENCES

[1] L.Giardino, F.Meo (edd.), “Prima di Muro. Dal villaggio iapigio alla città messapica”, Lecce 2011.

[2] L.Giardino, F.Meo (edd.), “Muro Leccese. Alla scoperta di una città messapica”, Lecce 2016.

[3] L.Giardino, P.Fabbri, M.T.Giannotta, L.Masiello, “Gruppi gentilizi in Messapia tra VI e III sec. a.C. Le sepolture di Muro Leccese (Puglia, Italia)”, in J.M.Álvarez, T.Nogales, I.Rodà (edd.), “Centre and Periphery in the Ancient World”, Proceedings of the 18th International Congress of Classical Archaeology (Merida 2013), Merida 2014, pp. 419-424.

[4] L.Giardino, C.Bianco, F.Meo, “Muro Leccese (Puglia, Italia). Forme e funzioni delle ceramiche d’uso quotidiano in un centro messapico tra IV e III secolo a.C.”, in R.Roure (ed.), “Contacts et acculturations en Méditerranée Occidentale. Hommages à Michel Bats”, Actes du colloque (Hyères 2011), BiAMA 15, Aix-en-Provence 2015, pp. 357-365.

[5] F.Meo, “Ceramiche di importazione greca a Muro Leccese (VIII-VI sec. a.C.). Una nota”, Studi di Antichità 13, 2015, pp. 181-190.

[6] F.Meo, “Ceramica dell'età del Ferro”, in P.Arthur, B.Bruno, S.Alfarano (edd.), “Archeologia Urbana a Borgo Terra. Muro Leccese”, Firenze, 2017, pp. 73-79.

[7] F.Meo, “Ceramica di età Messapica”, in P.Arthur, B.Bruno, S.Alfarano (edd.), “Archeologia Urbana a Borgo Terra. Muro Leccese”, Firenze, 2017, pp. 80-86.

[8] M.Lombardo, “I Messapi e la Messapia nelle fonti letterarie greche e latine”, Galatina 1992, p. 84, n. 146

(Livius), pp. 146-147 n. 272 (Florus), p. 165 n. 301 (Justinus), p. 261 in addition to all the other literary sources on the *bellum sallentinum*.
[9] F.Grelle, M.Silvestrini, "La Puglia nel mondo romano. Storia di una periferia. Dalle guerre sannitiche alla guerra sociale", Pragmateiai 24, Bari 2013, pp. 115-125.
[10] L.Giardino, F.Meo, "Un decennio di indagini archeologiche a Muro Leccese. Il villaggio dell'età del Ferro e l'abitato arcaico", in G.Andreassi, A.Cocchiaro, A.Dell'Aglio (edd.), "Vetustis novitatem dare. Temi di antichità e archeologia in ricordo di Grazia Angela Maruggi", Taranto 2013, pp. 299-319.
[11] L.Giardino, F.Meo, "Attestazioni di pratiche rituali di età arcaica nell'abitato messapico di Muro Leccese (Le)", in L.Giardino, G.Tagliamonte (edd.), "Archeologia dei luoghi e delle pratiche di culto", Atti del Convegno (Cavallino 2012), Bibliotheca Archaelogica 32, Bari 2013, pp. 165-203, pls. XIX-XXIV.
[12] L.Giardino, "Cratere a volute attico a figure nere dal centro messapico di Muro Leccese (Puglia, Italia)", in J. De La Genière (ed.), "Le cratère à volutes. Destination d'un vase de prestige entre Grecs et non-Grecs", Cahiers du CVA 2, Paris 2014, pp. 215-223.
[13] This subject is attested on some lip-cups, i.e.: Boston, Museum of Fine Arts (69.1052); Cyrene, Museum (409.13); Frankfurt, Liebieghaus (528); Kurashiki Ninagawa Museum, Japan (25); New York, Metropolitan Museum of Art (17.230.5); Oxford, Ashmolean Museum (1966.941; 1972.162); Samos, Vathy Museum (K2599; K6791; K6925).
[14] This subject is attested on some lip-cups, i.e.: CVA Fiesole, Collezioni Costantini 1, 17. Pl. (2545) 331.1, 33.3; CVA Basel, Antikenmuseum 1,97, PL. (181) 35.5. 11-12.
[15] B.Shefton, "The Lancut Group. Silouette Tecnique and Coral Red", in M-C. Villanueva Puig, "Céramique et peinture Grecques mode d'emploi", Atti del Convegno tenuto all'Ecole di Louvre (26-28.04.1995), Paris 1999, pp.463-479.
[16] C.Lambrugo, "La ceramica attica in Apulia: una grande officina, i suoi pittori, un vaso famoso", in G.Sena Chiesa, F.Slavazzi (edd.), "Ceramiche attiche e magnogreche. Collezione Banca Intesa. Catalogo ragionato", Milano 2006, pp. 44-93.
[17] M.Mazzei, "Importazioni ceramiche e influssi culturali in Daunia nel VI e V secolo a.C.", Papers in Italian Archaeology IV (BAR IS 245), Oxford 1985, pp. 263-283.
[18] G.Semeraro, "En Neusi" (BACT 2), Lecce-Bari 1997.
[19] Corpus Vasorum Antiquorum, 1922-, Lecce III He, n.3.
[20] L.Giardino, F.Meo (edd.), "Prima di Muro. Dal villaggio iapigio alla città messapica", Lecce 2011, p. 22, fig. 55.
[21] Corpus Vasorum Antiquorum, 1922-, Lecce III He, tav. 1.4-2.5.
[22] J.D.Beazley, "Attic Black-Figure Vase-Painters", Oxford 1956, p. 565, n. 616 (from Ure K3 group R).
[23] A.San Pietro, "La ceramica a figure nere di San Biagio (Metaponto)", Galatina 1991.
[24] J.D.Beazley, "Attic Black-Figure Vase-Painters", Oxford 1956, pp. 538-583.
[25] G.Semeraro, "En Neusi" (BACT 2), Lecce-Bari 1997, footnote 10.
[26] http://www.shapegrabber.com
[27] http://www.innovmetric.com
[28] F.Blais, J.Taylor, L.Cournoyer, M.Picard, L.Borgeat, G.Godin, J.-A.Beraldin, M.Rioux, C.Lahanier, B.Mottin, "More than a poplar plank: the shape and subtle colors of the masterpiece Mona Lisa by Leonardo", Videometrics IX, Electronic Imaging, San Jose, CA, 2007, 649106 1-10.
[29] F.Blais, J.Taylor, L.Cournoyer, M.Picard, L.Borgeat, L.-G.Dicaire, M.Rioux, J.-A.Beraldin, G.Godin, C.Lahanier, G.Aitken, "Ultra-High Resolution Imaging at 50µm using a Portable XYZ-RGB Color Laser Scanner", Intl. Workshop on Recording, Modeling and Visualization of Cultural Heritage. Centro Stefano Franscini, Monte Verita. Ascona, Switzerland. 2005, May 22-27.
[30] S.Pasinetti, I.Bodini, M.Lancini, F.Docchio, G.Sansoni, "A Depth from Defocus Measurement System Using a Liquid Lens Objective for Extended Depth Range", IEEE Trans. on Instrum. and Meas., vol.66, No.3, March 2017, pp. 441 - 450.
[31] E.Nocerino, F.Menna, F.Remondino, J.-A.Beraldin, L.Cournoyer, G.Reain, "Experiments on calibrating tilt-shift lenses for close-range photogrammetry", XXIII ISPRS Congress, 12–19 July 2016, Prague, Czech Republic. pp. 99-105.
[32] E.R.Dowski and W. T. Cathy, "Extended depth of field through wave-front coding" Applied Optics 34 1859 – 1866 (1995).
[33] http://www.agisoft.com/
[34] Commercial focus stacking software used in demo mode. http://www.heliconsoft.com/
[35] http://www.dxomark.com
[36] MA.Drouin, JA.Beraldin, "Active 3D Imaging Systems", in: Pears N., Liu Y., Bunting P. (eds) 3D Imaging, Analysis and Applications. Springer, London, 2012.
[37] In Beazley's vocabulary 'Class' refers to shape, 'Group' to style of drawing.
[38] P.N.Ure, "Sixth and Fifth Century Pottery from excavations made at Rhitsona by R. M. Burrows in 1909 and by P. N. Ure and A. D. Ure in 1921 and 1922", London 1927, pp.68-69.
[39] L.MacDonald, V.Moitinho de Almeida, M.Hess, "Three-dimensional reconstruction of Roman coins from photometric image sets", Journal of Electronic Imaging 26(1), 011017 (Jan/Feb 2017).